Heliyon 10 (2024) e39420

Contents lists available at ScienceDirect

Heliyon

journal homepage: www.cell.com/heliyon

Research article

Multi-omics analysis revealed significant metabolic changes in brain cancer cells treated with paclitaxel and/or topotecan

Ahlam M. Semreen [a,b], Leen Oyoun Alsoud [a,b], Mohammad H. Semreen [a,b], Munazza Ahmed [a,c], Hamza M. Al-Hroub [a], Raafat El-Awady [a,c], Wafaa S. Ramadan [a], Ahmad Abuhelwa [a,c], Yasser Bustanji [a,d,e], Nelson C. Soares [a,f,g,*], Karem H. Alzoubi [a,c,**]

[a] Research Institute of Medical and Health Sciences, University of Sharjah, Sharjah, 27272, United Arab Emirates
[b] Department of Medicinal Chemistry, College of Pharmacy, University of Sharjah, Sharjah, 27272, United Arab Emirates
[c] Department of Pharmacy Practice and Pharmacotherapeutics, College of Pharmacy, University of Sharjah, Sharjah, 27272, United Arab Emirates
[d] School of Pharmacy, The University of Jordan, Amman, 11942, Jordan
[e] Department of Basic and Clinical Pharmacology, College of Medicine, University of Sharjah, Sharjah, 27272, United Arab Emirates
[f] Center for Applied and Translational Genomics (CATG), Mohamed Bin Rashid University of Medicine and Health Sciences (MBRU), Dubai Health, Dubai, United Arab Emirates
[g] College of Medicine, Mohamed Bin Rashid University of Medicine and Health Sciences (MBRU), Dubai Health, Dubai, United Arab Emirates

ARTICLE INFO

Keywords:
Proteomics
Metabolomics
Brain Cancer
Therapy
Drug treatment

ABSTRACT

Glioblastoma (GBM) stands as the most common primary malignant brain tumor. Despite the best standard therapies, GBM survivors have a brief survival time, about 24 months on average. The treatment is troublesome because the cancer cells may not respond well to specific therapies as they grow within an extensive network of blood vessels. Our study aims to evaluate the impact of paclitaxel 5.3 μg/mL and topotecan 0.26 μM solely and in pairwise combination on the resultant metabolic and proteomic signatures of the U87 cell line while using the precise ultra-high-performance liquid chromatography quadrupole time-of-flight mass spectrometry (UHPLC-Q-TOF) analytical technology. The U87 cells wear treated with DMSO, paclitaxel 5.3 μM, topotecan 0.26 μM, and their combinations. Using One-way ANOVA, we observed 14 significantly altered metabolites compared to those cells treated with DMSO. For combination treatment (paclitaxel and topotecan), 11 metabolites were significantly dysregulated. Sparse partial least squares-discriminant analysis (sPLS-DA) revealed minimal overlap, highlighting distinctions among the four groups. While for proteomics, a total of 79 proteins were significantly dysregulated among the groups. These findings can aid in identifying new biomarkers associated with the utilized drugs and creating a map for targeted therapy. EIF3F, GNB2L1, HINT2, and RPA3 were shown to be significantly upregulated in the combination group relative to the control. Moreover, ribosome, apoptosis, HIF-1 signaling, arginine and proline, glutathione, purine metabolism, apelin signaling pathway, and glycolysis were significantly altered in the combination group. Overall, this study underscores the effectiveness of multi-omics approaches in revealing the molecular mechanisms driving chemotherapy responses in cancer cells. Additionally, this work generates a

* Corresponding author. Research Institute of Medical and Health Sciences, University of Sharjah, Sharjah, 27272, United Arab Emirates.
** Corresponding author. Research Institute of Medical and Health Sciences, University of Sharjah, Sharjah, 27272, United Arab Emirates.
E-mail addresses: nelson.soares@dubaihealth.ae (N.C. Soares), kelzubi@sharjah.ac.ae (K.H. Alzoubi).

https://doi.org/10.1016/j.heliyon.2024.e39420
Received 9 July 2023; Received in revised form 14 October 2024; Accepted 14 October 2024
Available online 18 October 2024

comprehensive list of molecular alterations that can serve as a foundation for further investigations and inform personalized healthcare strategies to enhance patient outcomes.

1. Introduction

Brain tumors pose a significant challenge in oncology due to their aggressive nature and limited treatment options. Glioblastoma (GBM) is the most prevalent primary malignant brain tumor, accounting for almost 60 % of all gliomas and half of primary malignant tumors in the central nervous system (CNS) [1]. These tumors are predominantly composed of astrocytes [2], and affect the cerebral hemispheres, though they can also occur less commonly in the cerebellum, brainstem, or spinal cord [3,4]. Although GBM may occur at any age, they are more common in adults aged 45 to 75 [2]. The standard treatment for high-grade gliomas consists of surgical removal, concurrent radiation therapy, and a 6 week course of temozolomide (TMZ), followed by an additional 6 months of adjuvant TMZ [5]. Despite the best standard therapies, GBM survivors have a brief survival time, about 24 months on average [6]. Furthermore, GBM is challenging to remove entirely surgically because they have finger-like projections, especially when they grow near critical areas of the brain [7]. In addition, treatment is troublesome because the cancer cells may not respond well to specific therapies and their growth within an extensive network of blood vessels render them resistant to chemotherapeutics [8].

A multi-omics approach, which provides information on biomolecules across multiple layers appears promising for systematically and holistically understanding complex biological systems [9]. Currently, proteomics (studying proteins in large quantities) and metabolomics (studying small molecules and metabolites) are two emerging and growing fields that promise to reveal more about disease processes by investigating changes within cells, biofluids, or tissues [10]. Proteomics analysis can be utilized to comprehend disease processes, give disease diagnosis and prognosis, aid in medication development, and provide the foundation for biological discovery [10–12]. In addition, emerging metabolomics technology offers new insights into diseases' mechanisms by identifying disease-associated markers and tracking cellular metabolomic changes in response to therapies [13,14]. When integrated, these approaches can offer a comprehensive view of disease pathology.

Indeed, a combined analysis of treatment-naïve GBMs' genomic, post-translational modification, proteomic, and metabolomic datasets revealed insights into the biology of GBMs by highlighting critical phosphorylation events which facilitate oncogenic pathway activation [15,16]. Mass spectrometry (MS), which enables the identification of hundreds of molecules across numerous samples, has recently been used extensively in oncology to advance metabolomics and proteomics. When combined with genomic information, these techniques can provide an even deeper understanding of tumor biology, identifying new biomarkers and potential therapeutic targets [17].

In our previously published study, significant metabolic pathways were altered upon treatment of U87 and U373 cells with paclitaxel and/or etoposide [18]. Elsewhere, paclitaxel was found to have a strong apoptosis-inducing effect on GBM cells with increased penetration into the brain tumor [19,20]. However, further investigations can aid in exploring the precise impact of anticancer drugs on GBM at the molecular level. Topotecan is a topoisomerase 1 inhibitor mainly used for ovarian, cervical and small-cell lung cancers [21]. Interestingly, topotecan's ability to cross the blood-brain barrier suggests its potential as an effective treatment for brain cancer [22]. Topotecan, when used in combination with radiation, has been shown to improve survival outcomes in GBM patients compared to radiotherapy alone [23]. More recently, topotecan was found to be both safe and effective for patients with recurrent GBM [24]**.** However, an in-vitro study showed brain tumor growth decreased and survival was further improved using multi-agent treatment regimens of topotecan or doxorubicin coupled with methotrexate and vincristine compared to single treatments [25].

Our current study thus aims to investigate the effect of anticancer medications (paclitaxel 5.3 μg/mL and topotecan 0.26 μM) solely and in pairwise combination on the metabolic and proteomic changes within the U87 cell line while employing UHPLC -QTOF) mass spectrometry.

Such a multi-omics approach can aid in identifying new biomarkers associated with the drugs and create a map for targeted therapy. This personalized approach, has the potential to augment the precision and efficacy of treatments while minimizing adverse effects by focusing on the molecular vulnerabilities at the proteomic and metabolomic levels unique to each patient after treating with paclitaxel and/or etoposide.

2. Methodology

2.1. Reagents

Topotecan and paclitaxel were purchased from Merck (Darmstadt, Germany). The U87 cell line was obtained from the Radiobiology and Experimental Radio Oncology Lab, University Cancer Center Hamburg, Hamburg University, Hamburg, Germany. Fisher Chemical provided formic acid and Trifluoroacetic acid (Loughborough, UK). Honeywell (Seelze, Germany) supplied LC-MS CHROMASOLV, acetonitrile (ACN), deionized water, and Methanol (99.9 %). Disposables and reagents for protein preparation such as C18 tips and Lysyl Endopeptidase LysC, were provided by ThermoScientific (Rockford, USA). Bovine Serum Albumin and Bradford's reagent were sourced from Sigma-Aldrich (Louis, USA), and 37 % hydrochloric acid was acquired from VWR chemicals (France).

2.2. Cell line and culture

The U87 cell line, being one of the most widely utilized and well-characterized brain cancer cell lines [26], was selected as the in vitro model for this study. U87 cell line was obtained as a gift from the drug design & discovery lab - Research Institute for Medical and Health Sciences - University of Sharjah. This investigation used the DMEM medium supplemented with 10 % fetal bovine serum and 1 % penicillin/streptomycin to cultivate the U87 cell line as monolayers Sigma-Aldrich (Louis, USA). All cultures were grown at 37 °C in a humid environment with 5 % CO_2.

2.3. Cell treatment

Two million cells were seeded into each 75 cm^2 tissue culture flask for each treatment condition and analysis (metabolomics and proteomics) and incubated for 24 h. The cells were subsequently given a 24-h treatment of paclitaxel 5.3 μM and/or topotecan 0.26 μM. These concentrations were chosen based on previous studies [27].

2.4. Combined extraction process

Our extraction procedure was conducted similarly to the methods outlined in our previously published studies [18,20,28–30]. Briefly, 400 μL of lysis buffer solution was added to each sample. The samples were then left to rest for 10 min before being transferred into 10 mL tubes, followed by vortexing sonication at 30 % amplification in an ice bath. Samples were then centrifuged at 14,000 rpm for 5 min, and the supernatant was combined with methanol and chloroform, vortexed, and centrifuged again. The upper layer was carefully transferred to a new glass vial, followed by the addition of 300 μL of methanol until the resultant protein disk precipitated. The supernatant was transferred into separate glass vials for metabolomics analysis, and the precipitated white disk after centrifugation was dried, and resuspended in denaturation buffer. Protein quantification was completed using the Bradford assay.

Protein samples (100 μg proteins in 100 μL denaturation buffer) were prepared for LC-MS/MS analysis via in-soluble digestion. Samples were reduced with 10 mM dithiothreitol (DTT), alkylated with 55 mM iodoacetamide (IAA), and adjusted to pH 8.0 as needed. Predigestion with Lysyl Endopeptidase LysC (1:100 ratio) was followed by dilution with 20 mM ammonium bicarbonate and digestion with trypsin (1:100 ratio) overnight. Peptides were desalted using C18 tips, dried, and reconstituted in 1 % TFA. Elution was performed with 60 % ACN and 0.1 % formic acid (FA), after which peptides were dried (EZ-2 Plus, Gene-Vac-Ipswich, UK) and dissolved in 2 % ACN and 0.1 % FA for nanoLC-QTOF-MS proteomic analysis.

2.5. High-performance liquid chromatography Tandem mass spectrometry (HPLC–MS/MS)

A QTOF-MS system and Elute UHPLC with a Hamilton® Intensity Solo C18 column (100 mm × 2.1 mm, 1.8 μm beads) (Bruker Daltonik) was used to separate and detect metabolites and peptides. Inline reversed-phase chromatography was performed with solvent A (0.1 % formic acid in HPLC-grade water) and solvent B (0.1 % formic acid in acetonitrile) within the cells (Bruker, Bremen, Germany). Analyses utilized Trapped Ion Mobility Spectroscopy and an Apollo II electrospray ionization (ESI) source was used.

For metabolomics analysis, the column was maintained at 35 °C and for proteomics at 32 °C using the nano-flow-based HPLC systems. Metabolomics samples were injected twice, eluted over a 30-min gradient (1 %–99 % ACN), and re-equilibrated to 1 % ACN with flow rates of 250 and 350 μL/min for elution and re-equilibration, respectively. The drying gas was set at 10 μL/min, drying temperature at 220 °C, and nebulizer pressure at 2.2 bar. For proteomics, the scan range was 150–2200 *m/z*, while metabolomics was set at 20–1300 *m/z*, both in Auto-MS/MS mode. Collision energies ranged from 23 to 65 eV with a 3-s cycle in proteomics and 20 eV with a 0.5-s cycle in metabolomics. Sodium formate served as the calibrant in the initial 0.3 min of each run. Peptide elution was achieved using a gradient from 5 % to 95 % ACN over 95 min at a flow rate of 300 μL/min under 350 bar back pressure.

Before analysis, mass calibration was performed using external mass calibration (10 mM sodium formate calibration solution). Bruker T-ReX LC-QTOF solution was employed to evaluate both the column and mass spectrometer performance. Separation by reversed-phase liquid chromatography (RPLC) and multipoint retention time calibration were performed using TRX-3112-R/MS certified human serum specifically for the Bruker T-ReX LC-QTOF solution, provided by Nova Medical Testing Inc. For metabolomics, 10 μL from each sample was pooled to create quality control (QC) samples.

2.6. Metabolomics data processing and analysis

Data processing was conducted using MetaboScape® 4.0 software (Bruker, Bremen, Germany). In the T-ReX 2D/3D workflow, molecular feature detection was optimized with an intensity threshold and peak duration limits. Mass recalibration was applied to a retention time range of 0–0.3 min, retaining only features present in a minimum of six samples per cell type. The MS/MS import method was configured for averaging. Bucketing parameters were set with a retention time range of 0.3–25 min and a mass range of 50 to 1000 *m/z*. For accurate identification, unknown compounds in the QTOF MS data were identified based on MS/MS spectra and retention time (RT). The Human Metabolome Database (HMDB) 4.0, a comprehensive metabolomics resource, was used to match compounds that passed screening, utilizing MS/MS data alone or in combination with RT as a reference for final compound selections. To identify metabolites, MS/MS spectra and retention times were mapped using HMDB 4.0. When multiple features matched a single database entry, filtering was done by selecting the entry with the highest annotation quality score (AQ score) for each metabolite, prioritizing alignment with factors such as retention time, MS/MS, *m/z* values, analyte list, msigma, and spectral library data [31,32].

Furthermore, metabolite data were saved as CSV files and integrated into the complete metabolomics platform MetaboAnalyst 5.0 software (https://www.metaboanalyst.ca). For each drug, two-tailed independent student t-tests were employed to identify significantly different metabolites from DMSO. For each condition, box plots illustrating statistical significance and fold change for metabolite dysregulation was created. We used the one-way analysis of variance (ANOVA) to compare multiple groups. The threshold for significance was fixed at $p < 0.05$. Using the software MetaboAnalyst 5.0, Principal Component Analysis (PCA) was also performed to visualize the overall variation and clustering of the samples. The false discovery rate (FDR) was used to eliminate false positives and correct for multiple hypothesis testing. Enrichment analysis, joint pathway analysis, and heatmaps were also created using MetaboAnalyst.

2.7. Proteomics data processing

Proteins and peptides were identified using the Uniprot proteome for *Homo sapiens* and the Andromeda search engine, with the raw data processed utilizing MaxQuant 1.6.17.0 (https://www.maxquant.org/) [31,32]. For modifications, methionine oxidation, and N-terminal acetylation, were set as variable modifications, and carbamidomethylation of cysteine residues was appointed as a fixed modification. One unique peptide per protein and 2 peptides were required for protein group identification. All other parameters were set to their default values. A false discovery rate (FDR) of 1 % was applied to PSMs and protein group assignments. The precursor mass tolerance for PSMs was set at 20 ppm. The MaxLFQ algorithm was utilized for label-free quantification (LFQ) and in silico digestion followed the standard trypsin/P cleavage rule [32,33].

2.8. Proteomics statistical analysis

Perseus software version 2.0.5.0 [34] was utilized; proteins identified as potential contaminants were removed from the data, as were proteins that could only be recognized by their location and were reverse engineered. The LFQ values were log 2-transformed (x). Annotated proteins were filtered to keep only those with a minimum of 70 % correct values. As a next step, missing values were imputed using a normal distribution with a downshift of 1.8 and width of 0.3, each calculated independently for each sample. After

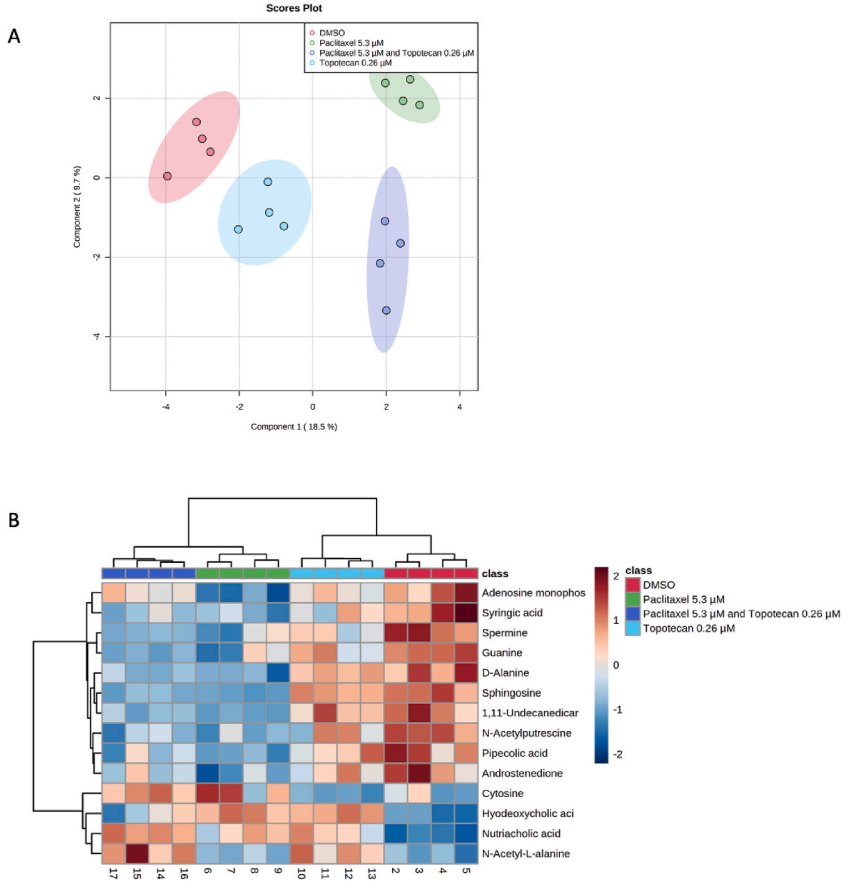

Fig. 1. (A)The sparse partial least squares discriminant analysis (sPLS-DA) for DMSO with paclitaxel 5.3 μM, DMSO with topotecan 0.26 μM, and DMSO with (paclitaxel 5.3 μM + topotecan 0.26 μM); (B) Heatmap for all the metabolites.

imputation, the data was analyzed using PCA. The proteins significantly expressed in the U87 cell line were determined using a two-tailed independent student *t*-test. Next, the Benjamini-Hochberg method was used to compensate for multiple testing. Proteins were determined to have differential expression when their log2 fold change was greater than 1 and the adjusted *p*-value was less than 0.05. The expression levels of differentially expressed proteins were compared between groups using hierarchical clustering, and the results were shown using a heatmap. Figures were generated via *R* software. Our parameters for data processing and analyses were employed similarly to those outlined in our previously published studies [18,20,28–30].

The metabolomic dataset has been deposited into a publicly available through **Workbench- Metabolomics** with the following details; **Project accession:** (datatrack_id:4804 study_id:ST003194); DOI: https://doi.org/10.21228/M8H14D).

3. Results

3.1. Metabolomics

Sixteen cancer cell samples treated with paclitaxel and/or topotecan—specifically DMSO, paclitaxel at 5.3 μM, topotecan at 0.26 μM, and a combination of paclitaxel 5.3 μM with topotecan 0.26 μM—were analyzed twice using LC-QTOF MS, resulting in 16,000 identifiable metabolite features. Following filtration, 109 metabolites were detected in samples treated with paclitaxel 5.3 μM and/or topotecan 0.26 μM. Fig. 1A demonstrates the sparse partial least squares-discriminant analysis (sPLS-DA), which shows minimal overlaps, indicating a difference between the four groups. The heatmap in Fig. 1B shows the significantly altered metabolites in all the group.

We next observed 14 significantly altered metabolites in all the treatment groups compared to the control group (One-way ANOVA) (Table 1). Box plots were generated to express the significantly altered metabolites concerning fold change (set to 1.5). The Spermidine, Guanine, D-Alanine, 1,11-Undecanedioic acid and Sphingosine appear to show a pattern of downregulation in the combination therapy compared to DMSO and other single-drug treatments (Fig. 2B). Comparisons included paclitaxel at 5.3 μM against DMSO, topotecan at 0.26 μM versus DMSO, and the combination of paclitaxel (5.3 μM) with topotecan (0.26 μM) relative to DMSO. A total of 4 metabolites were shown to be statistically significant when comparing paclitaxel 5.3 μM group with DMSO (Fig. 2A). Adenosine monophosphate, guanosine, and sphingosine were shown to have a lower abundance when compared to DMSO, while hyodeoxycholic acid was shown to have an increased abundance (Fig. 2A). Moreover, for the DMSO with topotecan, only hyodeoxycholic acid was shown to have increased abundance (Fig. 2B). However, for combination treatment, 11 metabolites were significantly dysregulated. Sphingosine, inosine, spermine, glutathione, guanosine, nutriacholic acid, guanine, pyroglutamic acid, hypotaurine, and indoleacetic

Table 1
One way ANOVA for the groups.

	P- Value valuep. value	FDR	Tukey's HSD
Sphingosine	0.000000011	0.00000012	Paclitaxel 5.3 ¬μM-DMSO; Paclitaxel 5.3 ¬μM and Topotecan 0.26 ¬μM-DMSO; Topotecan 0.26 ¬μM-Paclitaxel 5.3 ¬μM; Topotecan 0.26 ¬μM-Paclitaxel 5.3 ¬μM and Topotecan 0.26 ¬μM
Nutriacholic acid	0.0000223	0.00093703	Paclitaxel 5.3 ¬μM-DMSO; Paclitaxel 5.3 ¬μM and Topotecan 0.26 ¬μM-DMSO; Topotecan 0.26 ¬μM-DMSO
D-Alanine	0.0000258	0.00093703	Paclitaxel 5.3 ¬μM-DMSO; Paclitaxel 5.3 ¬μM and Topotecan 0.26 ¬μM-DMSO; Topotecan 0.26 ¬μM-Paclitaxel 5.3 ¬μM; Topotecan 0.26 ¬μM-Paclitaxel 5.3 ¬μM and Topotecan 0.26 ¬μM
1,11Undecanedicarboxylic acid	0.0000509	0.0012628	Paclitaxel 5.3 ¬μM-DMSO; Paclitaxel 5.3 ¬μM and Topotecan 0.26 ¬μM-DMSO; Topotecan 0.26 ¬μM-Paclitaxel 5.3 ¬μM; Topotecan 0.26 ¬μM-Paclitaxel 5.3 ¬μM and Topotecan 0.26 ¬μM
Adenosine monophosphate	0.0000579	0.0012628	Paclitaxel 5.3 ¬μM-DMSO; Paclitaxel 5.3 ¬μM and Topotecan 0.26 ¬μM-Paclitaxel 5.3 ¬μM; Topotecan 0.26 ¬μM-Paclitaxel 5.3 ¬μM
Hyodeoxycholic acid	0.0000869	0.0015791	Paclitaxel 5.3 ¬μM-DMSO; Topotecan 0.26 ¬μM-DMSO; Paclitaxel 5.3 ¬μM and Topotecan 0.26 ¬μM-Paclitaxel 5.3 ¬μM; Topotecan 0.26 ¬μM-Paclitaxel 5.3 ¬μM and Topotecan 0.26 ¬μM
N-Acetyl-L-alanine	0.00010313	0.0016058	Paclitaxel 5.3 ¬μM and Topotecan 0.26 ¬μM-DMSO; Topotecan 0.26 ¬μM-DMSO; Paclitaxel 5.3 ¬μM and Topotecan 0.26 ¬μM-Paclitaxel 5.3 ¬μM; Topotecan 0.26 ¬μM-Paclitaxel 5.3 ¬μM
Spermine	0.00020101	0.0027388	Paclitaxel 5.3 ¬μM-DMSO; Paclitaxel 5.3 ¬μM and Topotecan 0.26 ¬μM-DMSO; Topotecan 0.26 ¬μM-DMSO
Guanine	0.00069777	0.0084507	Paclitaxel 5.3 ¬μM-DMSO; Paclitaxel 5.3 ¬μM and Topotecan 0.26 ¬μM-DMSO; Topotecan 0.26 ¬μM-Paclitaxel 5.3 ¬μM and Topotecan 0.26 ¬μM
Syringic acid	0.0011055	0.011182	Paclitaxel 5.3 ¬μM-DMSO; Paclitaxel 5.3 ¬μM and Topotecan 0.26 ¬μM-DMSO; Topotecan 0.26 ¬μM-DMSO
Pipecolic acid	0.0011284	0.011182	Paclitaxel 5.3 ¬μM-DMSO; Paclitaxel 5.3 ¬μM and Topotecan 0.26 ¬μM-DMSO; Topotecan 0.26 ¬μM-Paclitaxel 5.3 ¬μM
N-Acetylputrescine	0.0015605	0.014175	Paclitaxel 5.3 ¬μM-DMSO; Paclitaxel 5.3 ¬μM and Topotecan 0.26 ¬μM-DMSO
Cytosine	0.0049182	0.039835	Topotecan 0.26 ¬μM-Paclitaxel 5.3 ¬μM; Topotecan 0.26 ¬μM-Paclitaxel 5.3 ¬μM and Topotecan 0.26 ¬μM
Androstenedione	0.0051164	0.039835	Paclitaxel 5.3 ¬μM-DMSO

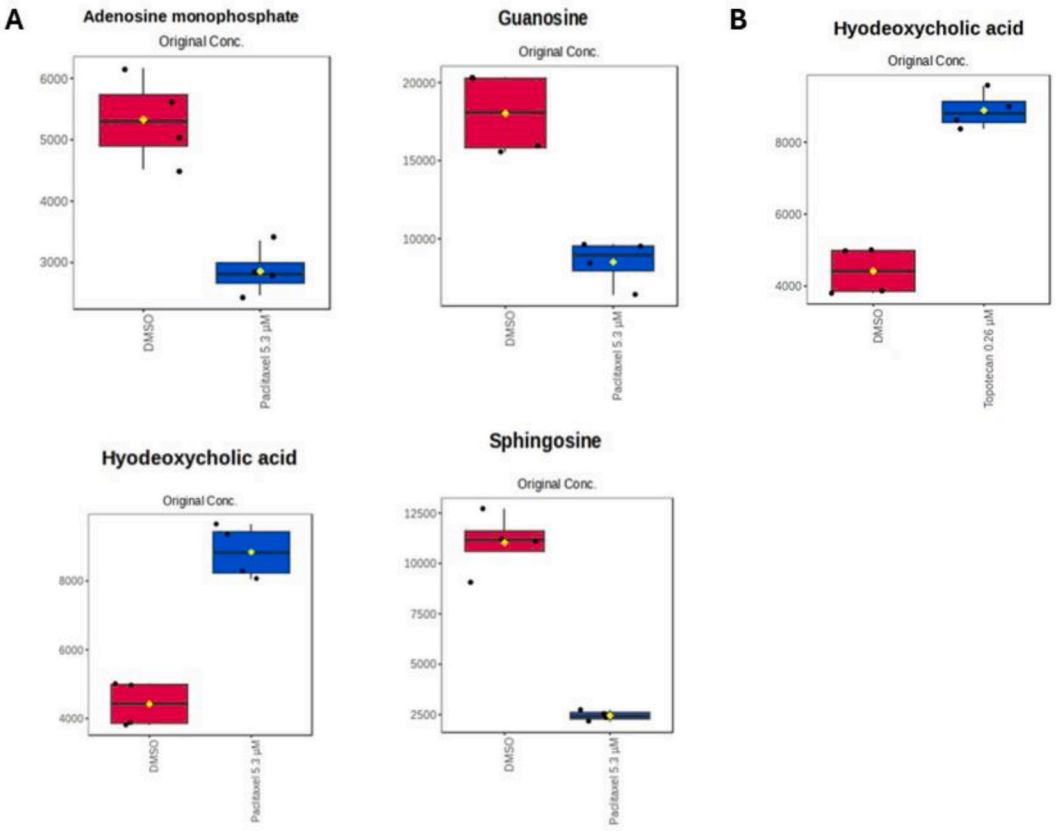

Fig. 2. Box plots for each significantly dysregulated metabolite in the (A) Paclitaxel and DMSO groups; (B) Topotecan and DMSO groups.

acid were reduced in abundance while cinnamic acid was increased in abundance (Fig. 3).

3.2. Enrichment analysis

Using the SMPBD database, significantly altered metabolites sets were subjected to pathway enrichment analysis in MetaboAnalyst 5.0. As shown in Fig. 4A and B, enrichment analysis included statistically significant metabolites ($p < 0.05$). Purine metabolism was highly enriched in both paclitaxel and combination treatments. However, thiamine metabolism, phenylacetaldehyde metabolism, alanine metabolism, and butyrate metabolism were specific to paclitaxel treatment. Glutathione metabolism, pyruvaldehyde degradation, taurine, and hypotaurine metabolism spermidine and spermine biosynthesis along with amino acid metabolism were significantly enriched in the combination treatment. However, for topotecan treatment, since hyodeoxycholic acid was the only significantly altered metabolite and it did not match the metabolite library set, no enrichment analysis could be performed.

3.3. Proteomics

A total of 66,651 spectra, 6663 peptides and 1023 proteins from these peptides were generated, after filtering for only those proteins identified by at least one unique and two total peptides. We subsequently filtered for those proteins with no missing values across all the samples, using the MaxQuant generated label-free quantification (LFQ) values, which resulted in 340 proteins with highly confident protein group assignments and quantitation for downstream analysis. The significantly altered proteins are mentioned in Table 1 in Supplement 1. Among the altered genes, P35244 (RPA3) was upregulated in topotecan treatment. Also, P62277 (RPS13) was found to be downregulated in paclitaxel and combination treatment. O15460 (P4HA2) was found to be downregulated in topotecan and combination treatment.

PCA shows the scattering of each group, suggesting that there are differences among the groups (Fig. 5A). This is supported by the distribution of coefficient of variance (CV) values for these proteins which shows that there is more variation across treatment groups than there is within the individual groups. However, the combination treatment introduces more variability within its group, likely due to complex interactions between the drugs (Fig. 5B). Among all the groups, 79 proteins were found to be significantly dysregulated in at least one group by ANOVA. Specifically, in the paclitaxel group, 46 were significantly impacted, while in topotecan, 27 were significantly dysregulated. In the combination group, 57 were shown to be significantly altered compared to the control (Table 1 in Supplement 1). Furthermore, the heatmap depicted in Fig. 5C shows complete separation of the groups confirming the difference

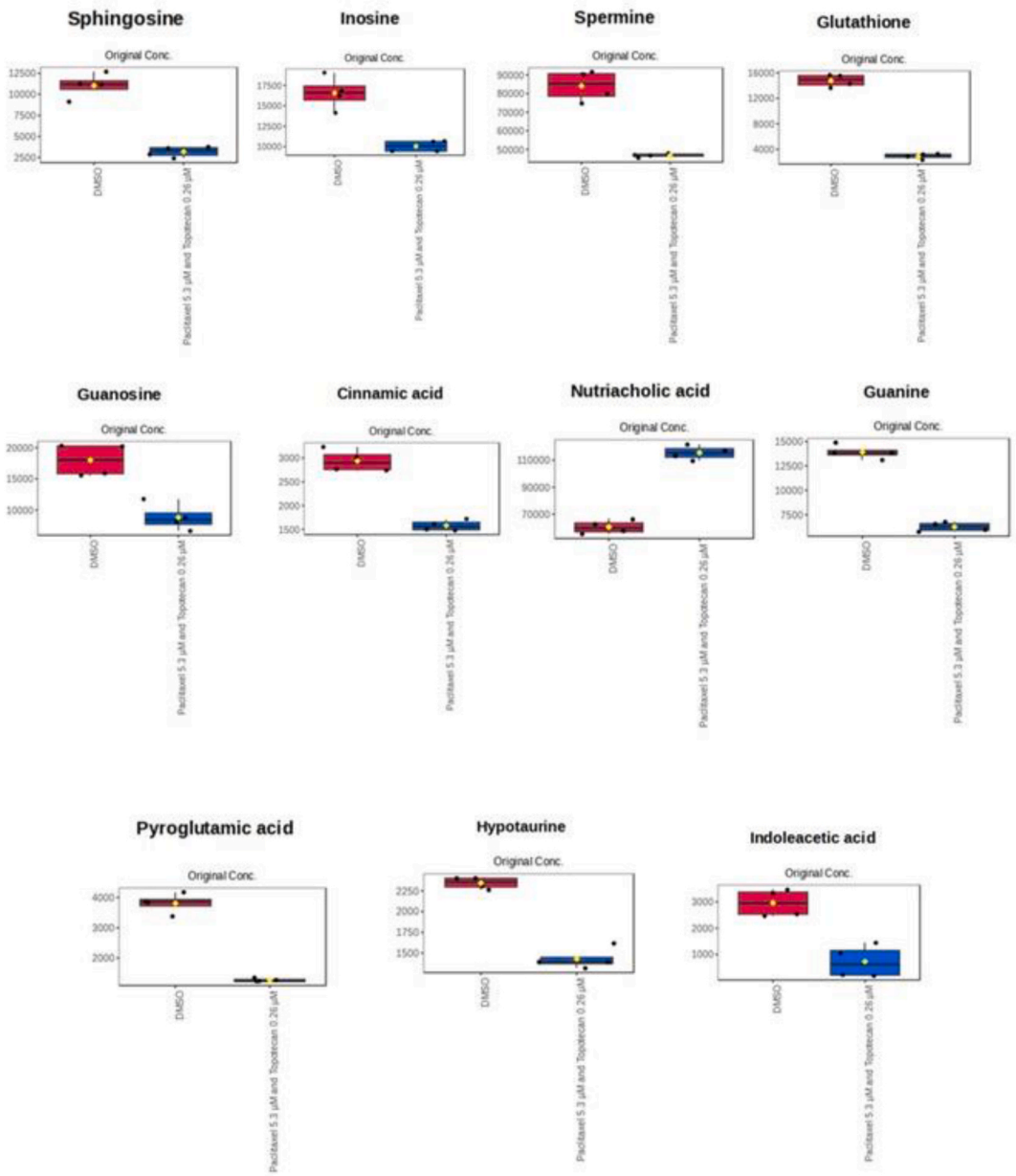

Fig. 3. Box plots for combination treatment (paclitaxel and topotecan).

among them. EIF3F and GNB2L1, RPA3, HINT2, and RPA3 were shown to be significantly upregulated in the combination group when compared to the control. While FDXR, RPL7, RPS3, and PSMB6 were significantly downregulated in the combination group compared to the control (Fig. 6). The HEXB protein was significantly upregulated upon the administration of topotecan treatment. The HMOX1 protein was significantly upregulated upon administering paclitaxel treatment, while SNRNP70 was downregulated.

3.4. Gene set enrichment analysis

The enriched biological processes from enrichment analyses are displayed in Fig. 7. The nodes are colored based on their adjusted *p* values and sized according to the number of proteins in the data which are part of the set. The x-axis indicates the Normalised Enrichment Score (NES) for the terms which were significantly altered. The NES represents whether the proteins in the indicated set are being collectively up- or downregulated (positive/negative).

Fig. 8 shows the integrated metabolomics and proteomics pathway analysis for the monotherapies and combination treatment. In the cells treated with paclitaxel, ribosome, protein processing in the endoplasmic reticulum, hypoxia-inducible factor 1 (HIF-1)

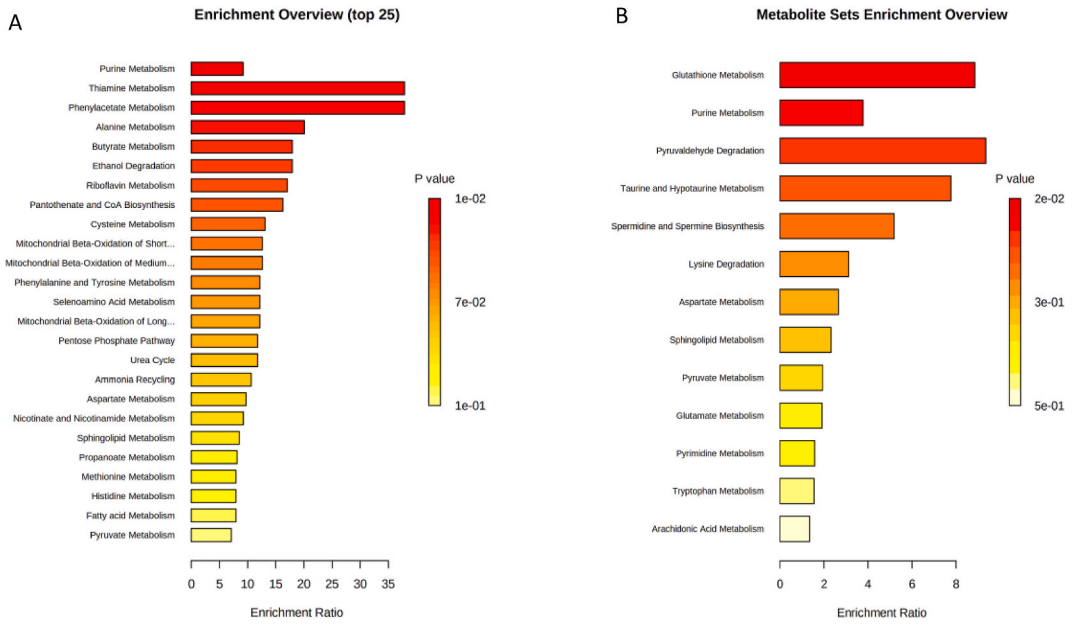

Fig. 4. Enrichment analysis for (A) DMSO with paclitaxel 5.3 μM; (B) DMSO with (paclitaxel 5.3 μM + topotecan 0.26 μM).

signaling pathway, Parkinson's disease, thermogenesis, glycolysis, and fructose and mannose metabolism were significantly perturbed. However, in topotecan treatment, lysosome, spliceosome, mismatch repair, DNA replication, phototransduction, apelin signaling pathway, and glycosphingolipid biosynthesis were significantly impacted. Moreover, in the combination group, ribosome, apoptosis, HIF-1 signaling, arginine and proline, glutathione, purine metabolism, apelin signaling pathway, and glycolysis were significantly altered. Other pathways impacted in combination treatment were vesicle lumen, secretory granule lumen, macromolecule biosynthesis process, and cellular macromolecule process.

4. Discussion

Paclitaxel, topotecan, and their combination treatment induces distinct metabolomic and proteomic signatures, with the combination more closely resembling that of paclitaxel. The PCA for the proteomics data, sPLS-DA for the metabolomics data, and hierarchical clustering for each (see Figs. 5A, 1A and 1B and 5C, respectively) together demonstrate a remarkably consistent pattern.

In the two-dimensional PCA and sPLS-DA analyses, topotecan and control treatments were observed to be clustering close to each other while paclitaxel clusters were far from control. This suggests that more considerable differences exist between control samples and paclitaxel-treated samples than with topotecan-treated samples. Additionally, we observe that samples treated with the combination of drugs cluster together, forming a distinct group with its own patterns of analyte abundance aside from their individual clusters.

Differentially abundant proteins were identified, showing associations with key cellular processes such as cell division, autophagy and apoptosis. Among these proteins, FDXR was significantly upregulated, and SERPINE1 was markedly downregulated following topotecan treatment. This finding aligns with their known functions: FDXR as a pro-apoptotic factor and SERPINE1 as a crucial player in the progression of GBM [35]. The downregulation of SERPINE1 by topotecan suggests its potential to inhibit GBM progression by targeting this specific pathway.

RPS3 was notably among the most significantly downregulated proteins following both paclitaxel and the combined treatment. This decrease is advantageous, as RPS3 is commonly overexpressed in cancer cells, and its downregulation may help mitigate tumorigenesis [36]. LDHA was one of the most strongly decreased proteins in all three treatments, suggesting metabolic pathways involved in cancer cell survival are effectively targeted. At the same time, others were related to cell cycle progression, differentiation, and immune cell development. Interestingly, HSP90B1, downregulated in topotecan, is a transcription factor involved in regulating neural development and differentiation. RPA3 has been shown to have both oncogenic and tumor-suppressive roles in different types of cancer, and its expression can be influenced by different factors, such as DNA damage, cell cycle regulation, and DNA replication stress [37].

At the pathway level, this same observation continues, with six pathways/GO terms being enriched for dysregulation in both the combination treatment and treatment with paclitaxel alone, showing the similarity between these two treatment regimes. Yet, while only three pathways showed significant enrichment from topotecan-only treatment in the proteomics data, all three pathways were likewise enriched in the combination treatment, indicating that mechanisms from topotecan treatment are present too.

This additive effect can be seen clearly in the proteomics data, where numerous proteins displayed synergistic or antagonistic interactions. Among the most significantly dysregulated proteins (Fig. 6), HINT2 and GNB2L1 each show a strong synergistic effect in

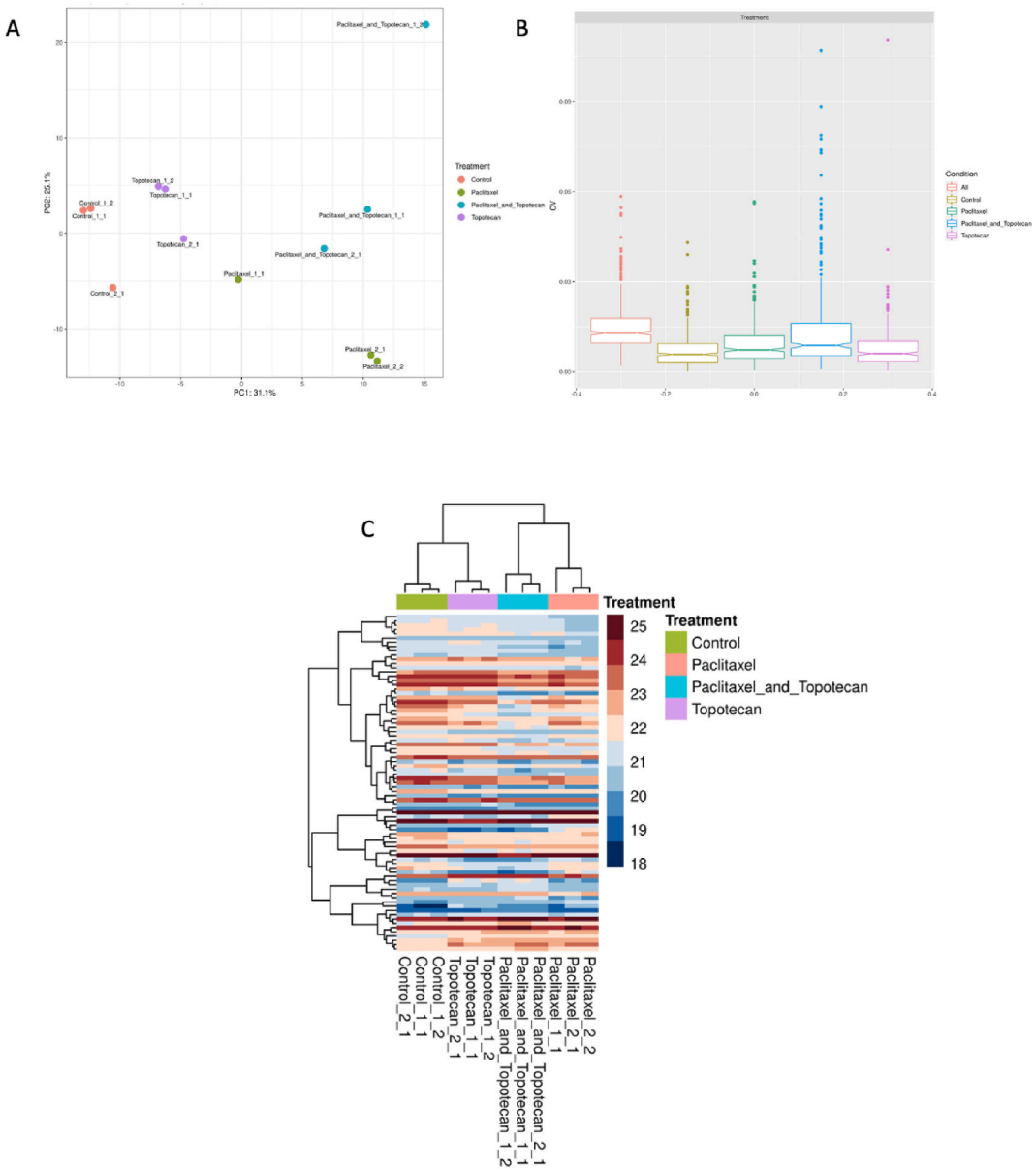

Fig. 5. A) Principal components analysis of the groups; B) Coefficient of variation of the proteins among the groups; C)Heatmap of all the groups.

the two treatments, both causing changes in the same direction, and this leading to an exponentially stronger dysregulation in the combined treatment (points are plotted on a logarithmic scale). These combined drug effects also lead to examples of negative synergy or antagonistic interactions such as that observed with HMOX1, which was the second most strongly (largest fold-change) increased protein upon paclitaxel treatment, yet no different from controls upon the combination with topotecan.

Yet, even more, surprising are those examples where some interaction between the drug effects leads not to a failed synergy – a decrease and increase combining to only a lesser increase or decrease – but a genuinely surprising antagonism between the treatments. This can be seen, for example, with hyodeoxycholic acid in the metabolomic data and JUP in the proteomic data. In both cases, the analyte was significantly increased upon treatment with either paclitaxel or topotecan. Hyodeoxycholic acid is a natural secondary bile acid [38]. Bile acids are derived from cholesterol, and glial cells, including U87 cells, are recognized for their capability to synthesize lipids such as fatty acids and cholesterol through de novo lipogenesis (DNL) [39,40]. However, byproducts of altered cholesterol pathways could lead to the production of bile acid derivatives like hyodeoxycholic acid [41,42]. This dysregulation may result from metabolic reprogramming in U87 cells in response to treatment with topotecan or paclitaxel, enabling the cells to support their growth and survival and resist the effects of the therapy [43]. Combination of the drugs shows a relatively downregulated expression of hyodeoxycholic acid (Fig. 1B). While a single drug alone might inadvertently increase the levels of this metabolite, potentially aiding

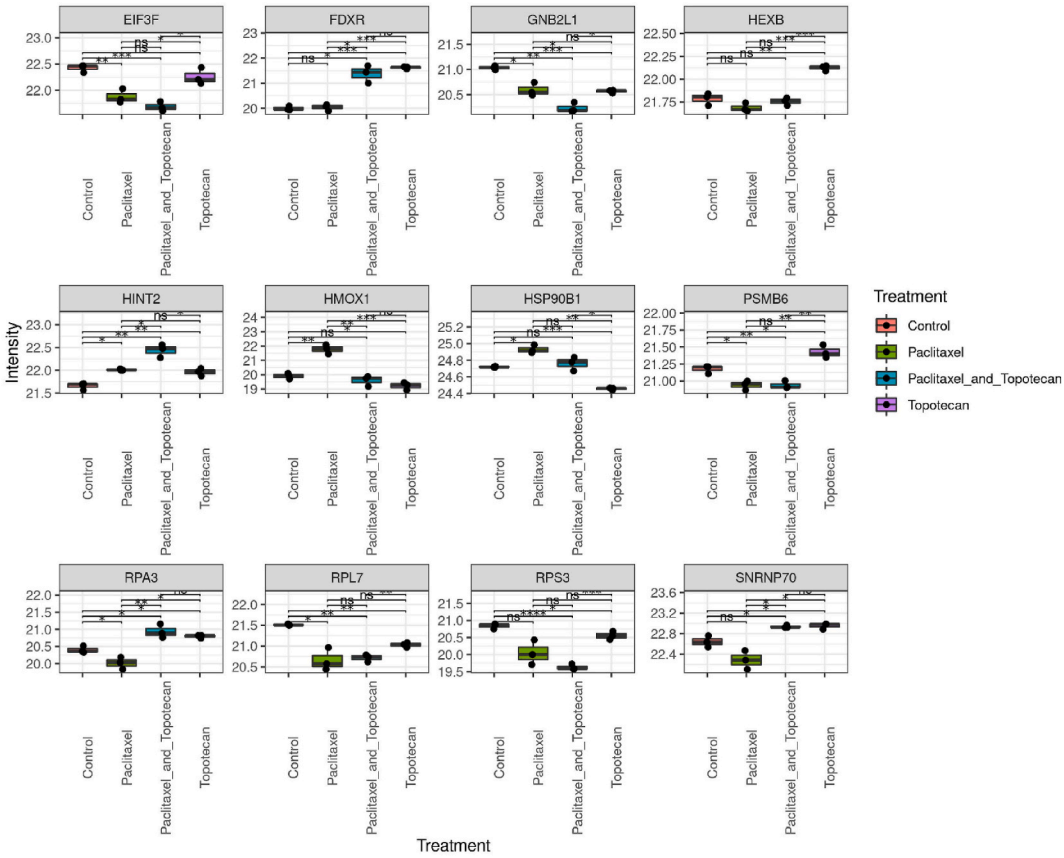

Fig. 6. Abundance profiles of the most significantly dysregulated proteins labelled by gene names.

cancer survival, combination therapy appears to counteract this effect. This suggests that the combination therapy could be more effective at inhibiting cancer growth by preventing the upregulation of harmful metabolites like hyodeoxycholic acid, thereby offering a more robust therapeutic outcome. Moreover, JUP, a structural and functional homolog of β-catenin [44], was explicitly the single most strongly increased protein upon either treatment, yet, upon a combination of the treatments, no significant difference can be observed. Thus, while the combined treatment appears to represent an addition of the two separate treatments predominantly, these examples of synergy and antagonism are essential in demonstrating that it nevertheless represents a distinct therapy, with sometimes synergistic, sometimes antagonistic, and sometimes outright surprising interaction effects and unique properties. The strong upregulation of JUP seen here could suggest a stress-induced mechanism promoting tumorigenesis [45]. However, the combination treatment's lack of significant JUP expression compared to control indicates that it may effectively counteract this stress response, preventing the compensatory upregulation of JUP. This suggests that the combination therapy might neutralize the tumor-promoting effects seen with individual treatments, offering a more balanced and effective approach.

Paclitaxel and topotecan work together to suppress HIF-1-mediated resistance and inhibit glycolysis. The enrichment for dysregulation in the hypoxia-inducible factor (HIF-1) pathway was seen in the proteomics gene set enrichment results for topotecan treatment, the joint-pathway metabolomic and proteomic analysis for paclitaxel treated samples, and both the gene set enrichment and joint-pathway analyses in the combination treatment. Thus, there is strong evidence that this pathway is affected by both treatments and the combination. Additionally, multiple downstream members of the regulon showed decreased abundance, including the previously mentioned HMOX1, SerpinE1, and LDHA. Alongside LDHA, the necessary glycolysis/gluconeogenesis enzymes PGK1 and ALDOA were likewise decreased, consistent with the role of HIF-1 in regulating glycolysis [46]. This relationship is particularly noteworthy as topotecan-treated samples revealed precisely three enriched protein pathways: HIF-1 signaling, glycolysis/gluconeogenesis, and COVID-19, where the last is perhaps a poorly named KEGG pathway with high overlap with ribosomal terms such as translation. With glycolysis/gluconeogenesis likewise being identified as an enriched term in topotecan and combination treatment, it is clear the HIF-1 signaling pathway is being suppressed and failing to upregulate glycolytic pathways upon treatment. As glycolysis is a pathway essential to cancer progression and upregulated in numerous cancers [47], the decreased abundance of these crucial enzymes upon treatment with anti-cancer drugs suggests that this dysregulation, likely mediated through the HIF-1 signaling pathway, forms an integral part of their respective mechanisms of action.

Previous studies [48] on the lung cancer cell lines PC14PE6 and NCI-H441 showed that the paclitaxel resistance observed in the former was due to constitutively higher base levels of HIF-1 alpha, and that hypoxia-induced HIF-1 alpha expression rendered both cell

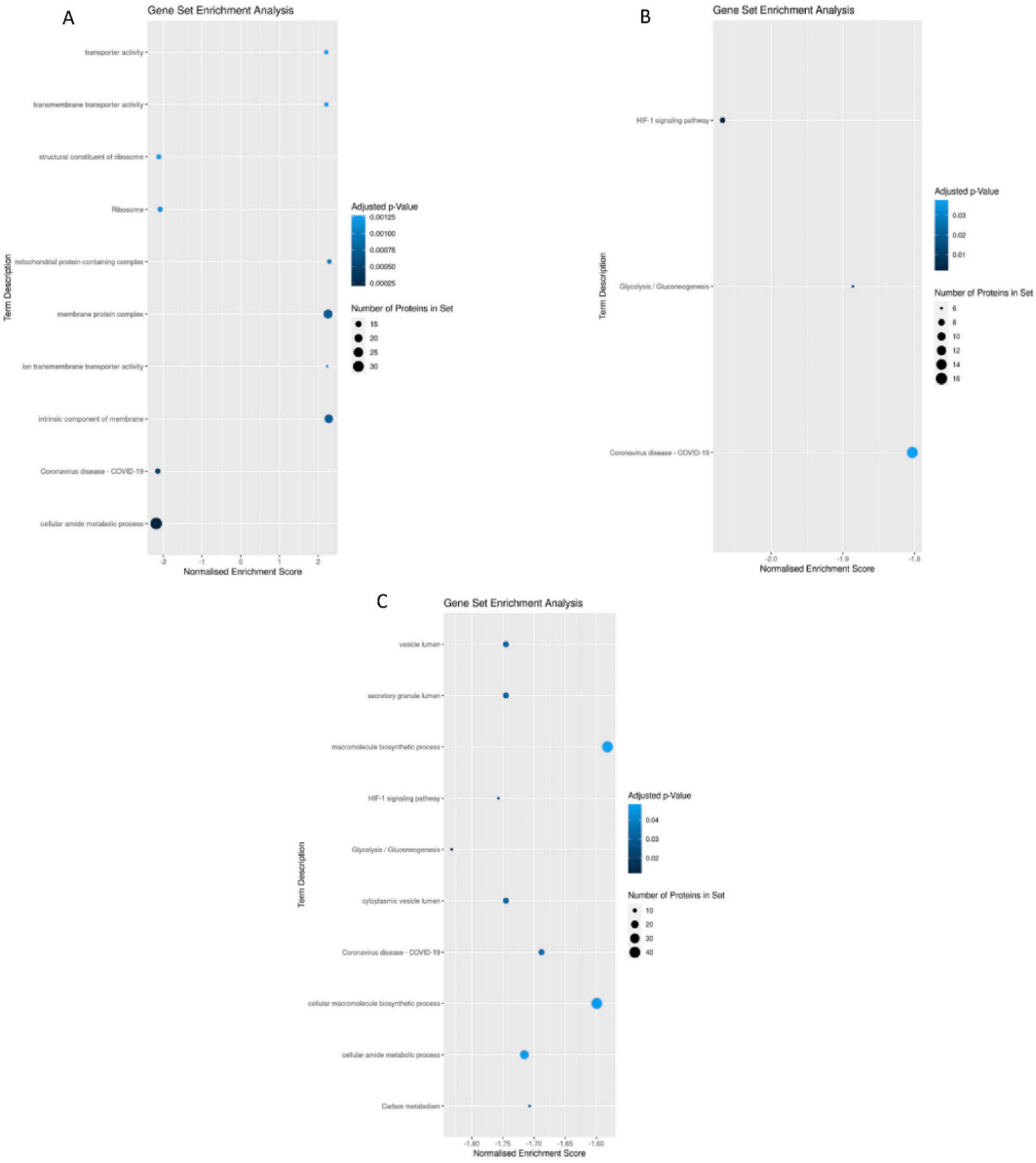

Fig. 7. Gene set enrichment analysis for A) Paclitaxel compared to control; B) Topotecan compared to control; C) Topotecan and paclitaxel compared to control.

lines resistant to paclitaxel. This could be mediated through HIF-1 alpha-induced overexpression of Tubulin [49], the target of paclitaxel, or through HIF-1 alpha-mediated resistance to apoptosis [50].

In our study, spermidine, guanine, D-Alanine, 1,11-Undecanediol and sphingosine were downregulated in the combination therapy compared to DMSO and other single-drug treatments. The interpretation of such findings lie in the context of metabolic reprogramming. For example, both Guanine (through nucleic acid metabolism) and spermidine (through polyamine metabolism) are crucial for cell proliferation [51,52]. 1,11-Undecanedioic acid and Sphingosine are connected to lipid metabolism, which is often reprogrammed in cancer cells to support rapid cell division [53]. In single drug treatments, upregulation might be related to altered metabolism to support uncontrolled growth, while downregulation in the combination highlights its potential to overcome metabolic reprogramming in favor of the malignancy. In fact, spermidine depletion has been reported to arrest mammalian cancer growth [54]. Although these metabolites are not part of a single linear pathway, they are part of broader networks that support key cellular functions such as membrane integrity and energy production. These networks can be co-regulated in response to stress upon single drug treatments, leading to coordinated changes in their levels.

Our one-way ANOVA shows that sphingosine, critical for cell signaling and membrane structure, displays significant differences between the paclitaxel-only group and both the DMSO control and combination therapy groups. This suggests that the combination

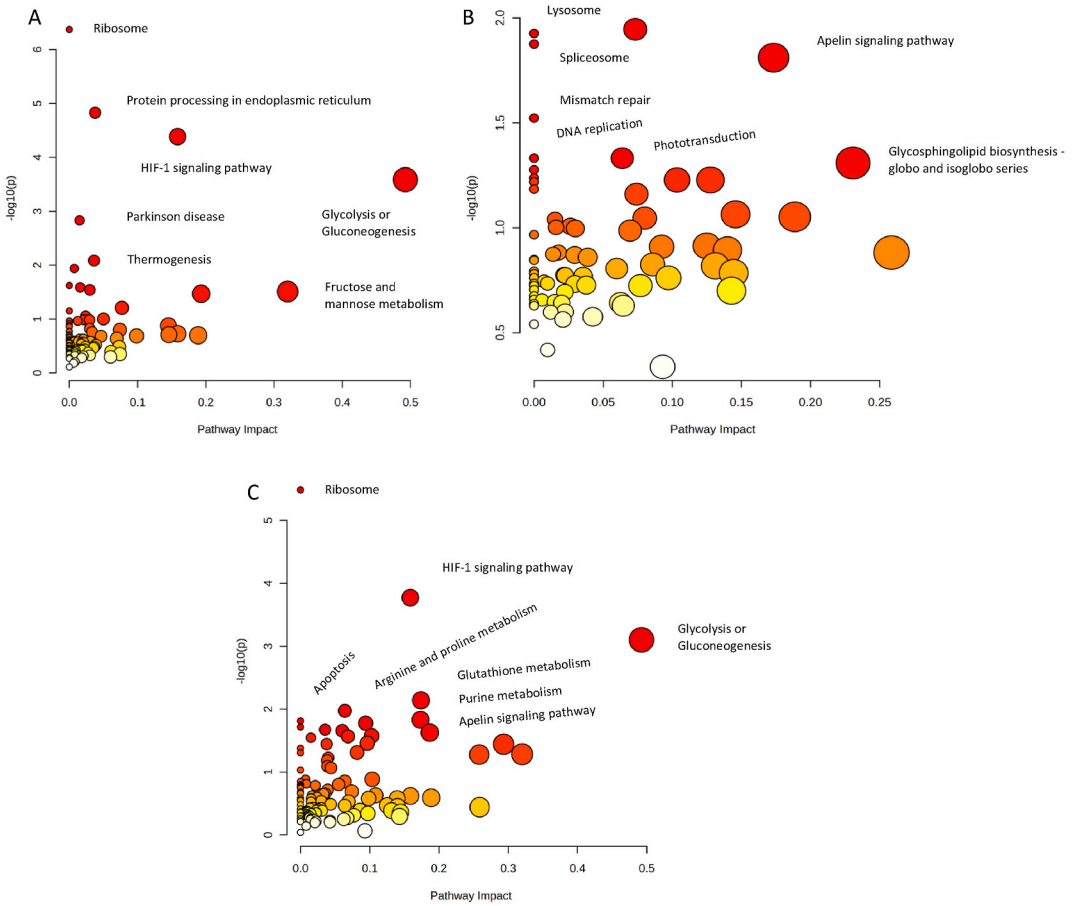

Fig. 8. Joint pathway analysis of metabolomics and proteomics for A) Cells treated with paclitaxel B) Cells treated with topotecan C) Cells treated with paclitaxel and topotecan.

therapy may modulate sphingolipid metabolism more effectively than paclitaxel alone. Similarly, guanine and spermidine, both of which are integral to nucleic acid and polyamine metabolism respectively, show significant downregulation in the combination therapy compared to single-drug treatments, indicating a potential disruption of pathways that are crucial for cancer cell proliferation. Moreover, metabolites like hyodeoxycholic acid and nutriacholic acid, which are associated with cholesterol and bile acid metabolism, also demonstrate significant changes, particularly between paclitaxel and combination therapy. This further supports the notion that combination therapy induces more comprehensive metabolic reprogramming, potentially enhancing its therapeutic efficacy by overcoming the metabolic adaptations that cancer cells may develop in response to single-drug treatments.

The joint pathway analysis (Fig. 8) highlights several significantly altered pathways across different conditions. A notable observation is the involvement of pathways such as the ribosome, HIF-1 signaling, glycolysis/gluconeogenesis, and glutathione metabolism across the different treatments. This suggests a potential upstream-downstream relationship where the ribosome and HIF-1 signaling pathways could serve as upstream regulators, influencing downstream processes like glycolysis/gluconeogenesis and glutathione metabolism.

Given that drug resistance often contributes to paclitaxel treatment failure, it was previously proposed that this drug be paired with treatments that target HIF-1 alpha [48]. Our data presented here, when combining the metabolomic and proteomic results, reveal the dysregulation of HIF-1 and glycolysis/gluconeogenesis to be present in paclitaxel treatment and, most importantly, in the combination treatment, confirming that the interactions between these two treatments are favorable in subduing the HIF-1 signaling pathway dysregulation and suggesting that this treatment combination would indeed be less susceptible to the emergence of paclitaxel drug resistance.

In our subsequent research, we plan to incorporate differential proteomic analysis both before and after treatment interventions, such as those with paclitaxel and/or topotecan, to further elucidate the specific changes in protein expression related to GBM treatment efficacy and mechanistic insights. Moreover, we intend to expand upon our current findings by implanting U87 cells into animal models to induce GBM. This forthcoming investigation will address the disparity between our laboratory-based observations and the effect of the tumor microenvironment. Such a strategy is anticipated to understand the molecular alterations of U87 cells within a realistic physiological setting, thereby facilitating a deeper understanding of GBM advancement and therapeutic efficacy.

CRediT authorship contribution statement

Ahlam M. Semreen: Writing – original draft, Visualization, Software, Investigation. **Leen Oyoun Alsoud:** Writing – original draft, Visualization, Validation, Software, Investigation, Formal analysis, Data curation. **Mohammad H. Semreen:** Writing – review & editing, Project administration, Methodology, Conceptualization. **Munazza Ahmed:** Writing – review & editing, Writing – original draft, Methodology, Investigation, Formal analysis, Data curation. **Hamza M. Al-Hroub:** Visualization, Validation, Software, Methodology, Formal analysis, Data curation. **Raafat El-Awady:** Methodology, Investigation. **Wafaa S. Ramadan:** Methodology. **Ahmad Abuhelwa:** Software, Methodology. **Yasser Bustanji:** Methodology, Data curation. **Nelson C. Soares:** Writing – review & editing, Writing – original draft, Visualization, Validation, Supervision, Resources, Project administration, Methodology, Investigation, Formal analysis, Data curation, Conceptualization. **Karem H. Alzoubi:** Writing – review & editing, Writing – original draft, Supervision, Resources, Investigation, Funding acquisition, Data curation, Conceptualization.

Funding

This research was funded by University of Sharjah, grant numbers 2201110362.

Data availability

The proteomic dataset has been deposited into a publicly available through **PRIDE** with the following details- **Project Name:** *Multi-Omics Analysis Revealed Significant Metabolic Changes in Brain Cancer Cells Treated with Paclitaxel and/or Topotecan*; **Project accession:** PXD052027. The metabolomic dataset has been deposited into a publicly available through Workbench- Metabolomics with the following details; Project accession: (datatrack_id:4804 study_id:ST003194); DOI: https://smex-ctp.trendmicro.com:443/wis/clicktime/v1/query?url=http%3a%2f%2fdx.doi.org%2f10.21228%2fM8H14D&umid=40487e3d-858d-4a8f-a859-aae55a83f1ed&auth=c59bb4781a3ce89e735bfc1f59bf1491d29edcb3-178481352ff88725eac2f81faf588a1f606d59d4.

Declaration of competing interest

The authors declare that they have no known competing financial interests or personal relationships that could have appeared to influence the work reported in this paper.

Appendix A. Supplementary data

Supplementary data to this article can be found online at https://doi.org/10.1016/j.heliyon.2024.e39420.

References

[1] Q.T. Ostrom, G. Cioffi, H. Gittleman, N. Patil, K. Waite, C. Kruchko, J.S. Barnholtz-Sloan, CBTRUS statistical report: primary brain and other central nervous system tumors diagnosed in the United States in 2012-2016, Neuro Oncol. 21 (2019) v1–v100, https://doi.org/10.1093/neuonc/noz150.
[2] Glioblastoma (GB) - brain tumour foundation of Canada. https://www.braintumour.ca/brain_tumour_types/glioblastoma-gb/, 2022.
[3] M. Etemadifar, S. Mousavi, M. Salari, S.A. Hosseinian, A.R. Mansouri, Whole spinal transverse myelitis in neuromyelitis optica spectrum disorder, Mult Scler Relat Disord 87 (2024) 105666, https://doi.org/10.1016/j.msard.2024.105666.
[4] W. Yuan, J. Sun, Q. Li, R. Zheng, B. Guan, Z. Chen, J. Ding, Q. Sun, R. Fu, W. Wang, Y. Fan, Y. Kang, C. Sun, A. Li, D. Wu, D. Wang, L. Qi, L. Chen, S. Feng, H. Zhou, Protocol for the Chinese Real-World Evidence for Acute Spinal Cord Injury (ChiRES) study: a prospective, observational, multicentre cohort study of acute spinal cord injury, BMJ Open 14 (2024) e080358, https://doi.org/10.1136/bmjopen-2023-080358.
[5] D. Khosla, Concurrent therapy to enhance radiotherapeutic outcomes in glioblastoma, Ann. Transl. Med. 4 (2016) 54, https://doi.org/10.3978/j.issn.2305-5839.2016.01.25.
[6] M. Koshy, J.L. Villano, T.A. Dolecek, A. Howard, U. Mahmood, S.J. Chmura, R.R. Weichselbaum, B.J. McCarthy, Improved survival time trends for glioblastoma using the SEER 17 population-based registries, J. Neuro Oncol. 107 (2012) 207–212, https://doi.org/10.1007/s11060-011-0738-7.
[7] A. Amelot, F. Baronnet-Chauvet, E. Fioretti, B. Mathon, P. Cornu, A. Nouet, D. Chauvet, Glioblastoma complicated by fatal malignant acute ischemic stroke: MRI finding to assist in tricky surgical decision, NeuroRadiol. J. 28 (2015) 483–487, https://doi.org/10.1177/1971400915598073.
[8] D.S. Tews, A. Nissen, C. Külgen, A.K.A. Gaumann, Drug resistance-associated factors in primary and secondary glioblastomas and their precursor tumors, J. Neuro Oncol. 50 (2000) 227–237, https://doi.org/10.1023/A:1006491405010.
[9] J. Yan, S.L. Risacher, L. Shen, A.J. Saykin, Network approaches to systems biology analysis of complex disease: integrative methods for multi-omics data, Briefings Bioinf. (2017), https://doi.org/10.1093/bib/bbx066.
[10] M. Kavallaris, G.M. Marshall, Proteomics and disease: opportunities and challenges, Med. J. Aust. 182 (2005) 575–579, https://doi.org/10.5694/j.1326-5377.2005.tb06817.x.
[11] A.A. Peyvandi, S. Khoshsirat, A. Safaei, M. Rezaei-Tavirani, M. Azodi-Zamanian, Interactome analysis of 11-dehydrosinulariolide-treated oral carcinoma cell lines such as Ca9-22 and CAL-27 and melanoma cell line, Int J Cancer Manag 10 (2017), https://doi.org/10.5812/ijcm.10096.
[12] A.G. Birhanu, Mass spectrometry-based proteomics as an emerging tool in clinical laboratories, Clin Proteomics 20 (2023) 32, https://doi.org/10.1186/s12014-023-09424-x.
[13] S. Qiu, Y. Cai, H. Yao, C. Lin, Y. Xie, S. Tang, A. Zhang, Small molecule metabolites: discovery of biomarkers and therapeutic targets, Signal Transduct Target Ther 8 (2023) 132, https://doi.org/10.1038/s41392-023-01399-3.
[14] A. Zhang, H. Sun, G. Yan, P. Wang, X. Wang, Metabolomics for biomarker discovery: moving to the clinic, BioMed Res. Int. 2015 (2015) 354671, https://doi.org/10.1155/2015/354671.

[15] S. Migliozzi, Y.T. Oh, M. Hasanain, L. Garofano, F. D'Angelo, R.D. Najac, A. Picca, F. Bielle, A.L. Di Stefano, J. Lerond, J.N. Sarkaria, M. Ceccarelli, M. Sanson, A. Lasorella, A. Iavarone, Integrative multi-omics networks identify PKCδ and DNA-PK as master kinases of glioblastoma subtypes and guide targeted cancer therapy, Nat. Can. (Ott.) 4 (2023) 181–202, https://doi.org/10.1038/s43018-022-00510-x.

[16] L.-B. Wang, A. Karpova, M.A. Gritsenko, J.E. Kyle, S. Cao, Y. Li, D. Rykunov, A. Colaprico, J.H. Rothstein, R. Hong, V. Stathias, M. Cornwell, F. Petralia, Y. Wu, B. Reva, K. Krug, P. Pugliese, E. Kawaler, L.K. Olsen, W.-W. Liang, X. Song, Y. Dou, M.C. Wendl, W. Caravan, W. Liu, D. Cui Zhou, J. Ji, C.-F. Tsai, V.A. Petyuk, J. Moon, W. Ma, R.K. Chu, K.K. Weitz, R.J. Moore, M.E. Monroe, R. Zhao, X. Yang, S. Yoo, A. Krek, A. Demopoulos, H. Zhu, M.A. Wyczalkowski, J.F. McMichael, B.L. Henderson, C.M. Lindgren, H. Boekweg, S. Lu, J. Baral, L. Yao, K.G. Stratton, L.M. Bramer, E. Zink, S.P. Couvillion, K.J. Bloodsworth, S. Satpathy, W. Sieh, S. M. Boca, S. Schürer, F. Chen, M. Wiznerowicz, K.A. Ketchum, E.S. Boja, C.R. Kinsinger, A.I. Robles, T. Hiltke, M. Thiagarajan, A.I. Nesvizhskii, B. Zhang, D. R. Mani, M. Ceccarelli, X.S. Chen, S.L. Cottingham, Q.K. Li, A.H. Kim, D. Fenyö, K.V. Ruggles, H. Rodriguez, M. Mesri, S.H. Payne, A.C. Resnick, P. Wang, R. D. Smith, A. Iavarone, M.G. Chheda, J.S. Barnholtz-Sloan, K.D. Rodland, T. Liu, L. Ding, Clinical proteomic tumor analysis consortium, proteogenomic and metabolomic characterization of human glioblastoma, Cancer Cell 39 (2021) 509–528.e20, https://doi.org/10.1016/j.ccell.2021.01.006.

[17] T. Kowalczyk, M. Ciborowski, J. Kisluk, A. Kretowski, C. Barbas, Mass spectrometry based proteomics and metabolomics in personalized oncology, Biochim. Biophys. Acta (BBA) - Mol. Basis Dis. 1866 (2020) 165690, https://doi.org/10.1016/j.bbadis.2020.165690.

[18] A.M. Semreen, L.O. Alsoud, W. El-Huneidi, M. Ahmed, Y. Bustanji, E. Abu-Gharbieh, R. El-Awady, W.S. Ramadan, M.A.Y. Alqudah, M. Shara, A.Y. Abuhelwa, N. C. Soares, M.H. Semreen, K.H. Alzoubi, Metabolomics analysis revealed significant metabolic changes in brain cancer cells treated with paclitaxel and/or etoposide, IJMS 23 (2022) 13940, https://doi.org/10.3390/ijms232213940.

[19] Y. Xu, M. Shen, Y. Li, Y. Sun, Y. Teng, Y. Wang, Y. Duan, The synergic antitumor effects of paclitaxel and temozolomide co-loaded in mPEG-PLGA nanoparticles on glioblastoma cells, Oncotarget 7 (2016) 20890–20901, https://doi.org/10.18632/oncotarget.7896.

[20] M. Haider, J. Jagal, K. Bajbouj, B.M. Sharaf, L. Sahnoon, J. Okendo, M.H. Semreen, M. Hamda, N.C. Soares, Integrated multi-omics analysis reveals unique signatures of paclitaxel-loaded poly(lactide-co-glycolide) nanoparticles treatment of head and neck cancer cells, Proteomics 23 (2023) e2200380, https://doi.org/10.1002/pmic.202200380.

[21] J.R. Diamond, B. Goff, M.D. Forster, J.C. Bendell, C.D. Britten, M.S. Gordon, H. Gabra, D.M. Waterhouse, M. Poole, D. Ross Camidge, E. Hamilton, K.M. Moore, Phase Ib study of the mitochondrial inhibitor ME-344 plus topotecan in patients with previously treated, locally advanced or metastatic small cell lung, ovarian and cervical cancers, Invest. N. Drugs 35 (2017) 627–633, https://doi.org/10.1007/s10637-017-0444-1.

[22] E.T. Wong, A. Berkenblit, The role of topotecan in the treatment of brain metastases, Oncol. 9 (2004) 68–79, https://doi.org/10.1634/theoncologist.9-1-68.

[23] G.G. Grabenbauer, K.-D. Gerber, O. Ganslandt, A. Richter, G. Klautke, J. Birkmann, M. Meyer, Effects of concurrent topotecan and radiation on 6-month progression-free survival in the primary treatment of glioblastoma multiforme, Int. J. Radiat. Oncol. Biol. Phys. 75 (2009) 164–169, https://doi.org/10.1016/j.ijrobp.2009.04.015.

[24] E.F. Spinazzi, M.G. Argenziano, P.S. Upadhyayula, M.A. Banu, J.A. Neira, D.M.O. Higgins, P.B. Wu, B. Pereira, A. Mahajan, N. Humala, O. Al-Dalahmah, W. Zhao, A.V. Save, B.J.A. Gill, D.M. Boyett, T. Marie, J.L. Furnari, T.D. Sudhakar, S.A. Stopka, M.S. Regan, V. Catania, L. Good, S. Zacharoulis, M. Behl, P. Petridis, S. Jambawalikar, A. Mintz, A. Lignelli, N.Y.R. Agar, P.A. Sims, M.R. Welch, A.B. Lassman, F.M. Iwamoto, R.S. D'Amico, J. Grinband, P. Canoll, J. N. Bruce, Chronic convection-enhanced delivery of topotecan for patients with recurrent glioblastoma: a first-in-patient, single-centre, single-arm, phase 1b trial, Lancet Oncol. 23 (2022) 1409–1418, https://doi.org/10.1016/S1470-2045(22)00599-X.

[25] C. Schmidt, N.A. Schubert, S. Brabetz, N. Mack, B. Schwalm, J.A. Chan, F. Selt, C. Herold-Mende, O. Witt, T. Milde, S.M. Pfister, A. Korshunov, M. Kool, Preclinical drug screen reveals topotecan, actinomycin D, and volasertib as potential new therapeutic candidates for ETMR brain tumor patients, Neuro Oncol. 19 (2017) 1607–1617, https://doi.org/10.1093/neuonc/nox093.

[26] M.T.C. Poon, M. Bruce, J.E. Simpson, C.J. Hannan, P.M. Brennan, Temozolomide sensitivity of malignant glioma cell lines – a systematic review assessing consistencies between in vitro studies, BMC Cancer 21 (2021) 1240, https://doi.org/10.1186/s12885-021-08972-5.

[27] J.E. Liebmann, J.A. Cook, C. Lipschultz, D. Teague, J. Fisher, J.B. Mitchell, Cytotoxic studies of paclitaxel (Taxol) in human tumour cell lines, Br. J. Cancer 68 (1993) 1104–1109, https://doi.org/10.1038/bjc.1993.488.

[28] B.M. Sharaf, A.D. Giddey, H.M. Al-Hroub, V. Menon, J. Okendo, R. El-Awady, M. Mousa, A. Almehdi, M.H. Semreen, N.C. Soares, Mass spectroscopy-based proteomics and metabolomics analysis of triple-positive breast cancer cells treated with tamoxifen and/or trastuzumab, Cancer Chemother. Pharmacol. 90 (2022) 467–488, https://doi.org/10.1007/s00280-022-04478-4.

[29] M. Ahmed, A.M. Semreen, A.D. Giddey, W.S. Ramadan, R. El-Awady, N.C. Soares, W. El-Huneidi, Y. Bustanji, M.A.Y. Alqudah, K.H. Alzoubi, M.H. Semreen, Proteomic and metabolomic signatures of U87 glioblastoma cells treated with cisplatin and/or paclitaxel, Ann. Med. 55 (2023) 2305308, https://doi.org/10.1080/07853890.2024.2305308.

[30] R.A. Zenati, A.D. Giddey, H.M. Al-Hroub, Y.A. Hagyousif, W. El-Huneidi, Y. Bustanji, E. Abu-Gharbieh, M.A.Y. Alqudah, M. Shara, A.Y. Abuhelwa, N.C. Soares, M.H. Semreen, Evaluation of two simultaneous metabolomic and proteomic extraction protocols assessed by ultra-high-performance liquid chromatography tandem mass spectrometry, IJMS 24 (2023) 1354, https://doi.org/10.3390/ijms24021354.

[31] L. Li, R. Li, J. Zhou, A. Zuniga, A.E. Stanislaus, Y. Wu, T. Huan, J. Zheng, Y. Shi, D.S. Wishart, G. Lin, MyCompoundID: using an evidence-based metabolome library for metabolite identification, Anal. Chem. 85 (2013) 3401–3408, https://doi.org/10.1021/ac400099b.

[32] J. Cox, M.Y. Hein, C.A. Luber, I. Paron, N. Nagaraj, M. Mann, Accurate proteome-wide label-free quantification by delayed normalization and maximal peptide ratio extraction, termed MaxLFQ, Mol. Cell. Proteomics 13 (2014) 2513–2526, https://doi.org/10.1074/mcp.M113.031591.

[33] J. Cox, M. Mann, MaxQuant enables high peptide identification rates, individualized p.p.b.-range mass accuracies and proteome-wide protein quantification, Nat. Biotechnol. 26 (2008) 1367–1372, https://doi.org/10.1038/nbt.1511.

[34] S. Tyanova, T. Temu, P. Sinitcyn, A. Carlson, M.Y. Hein, T. Geiger, M. Mann, J. Cox, The Perseus computational platform for comprehensive analysis of (prote) omics data, Nat. Methods 13 (2016) 731–740, https://doi.org/10.1038/nmeth.3901.

[35] G. Liu, X. Chen, The ferredoxin reductase gene is regulated by the p53 family and sensitizes cells to oxidative stress-induced apoptosis, Oncogene 21 (2002) 7195–7204, https://doi.org/10.1038/sj.onc.1205862.

[36] K. Pogue-Geile, J.R. Geiser, M. Shu, C. Miller, I.G. Wool, A.I. Meisler, J.M. Pipas, Ribosomal protein genes are overexpressed in colorectal cancer: isolation of a cDNA clone encoding the human S3 ribosomal protein, Mol. Cell Biol. 11 (1991) 3842–3849, https://doi.org/10.1128/mcb.11.8.3842-3849.1991.

[37] N.S. Gavande, P.S. VanderVere-Carozza, K.S. Pawelczak, T.L. Vernon, M.R. Jordan, J.J. Turchi, Structure-guided optimization of replication protein A (RPA)-DNA interaction inhibitors, ACS Med. Chem. Lett. 11 (2020) 1118–1124, https://doi.org/10.1021/acsmedchemlett.9b00440.

[38] Y. Tao, F. Zheng, D. Cui, F. Huang, X. Wu, A combination of three plasma bile acids as a putative biomarker for schizophrenia, Acta Neuropsychiatr. 33 (2021) 51–54, https://doi.org/10.1017/neu.2020.42.

[39] J.M. Dietschy, Central nervous system: cholesterol turnover, brain development and neurodegeneration, Biol. Chem. 390 (2009) 287–293, https://doi.org/10.1515/BC.2009.035.

[40] A.V. Garcia Corrales, M. Haidar, J.F.J. Bogie, J.J.A. Hendriks, Fatty acid synthesis in glial cells of the CNS, Int. J. Mol. Sci. 22 (2021) 8159, https://doi.org/10.3390/ijms22158159.

[41] C.A. Lewis, C. Brault, B. Peck, K. Bensaad, B. Griffiths, R. Mitter, P. Chakravarty, P. East, B. Dankworth, D. Alibhai, A.L. Harris, A. Schulze, SREBP maintains lipid biosynthesis and viability of cancer cells under lipid- and oxygen-deprived conditions and defines a gene signature associated with poor survival in glioblastoma multiforme, Oncogene 34 (2015) 5128–5140, https://doi.org/10.1038/onc.2014.439.

[42] S. Shakya, A.D. Gromovsky, J.S. Hale, A.M. Knudsen, B. Prager, L.C. Wallace, L.O.F. Penalva, H.A. Brown, B.W. Kristensen, J.N. Rich, J.D. Lathia, J.M. Brown, C. G. Hubert, Altered lipid metabolism marks glioblastoma stem and non-stem cells in separate tumor niches, Acta Neuropathol Commun 9 (2021) 101, https://doi.org/10.1186/s40478-021-01205-7.

[43] R. Pai, A.S. Tarnawski, T. Tran, Deoxycholic acid activates beta-catenin signaling pathway and increases colon cell cancer growth and invasiveness, Mol. Biol. Cell 15 (2004) 2156–2163, https://doi.org/10.1091/mbc.e03-12-0894.

[44] M.J. Buchmeier, R.M. Zinkernagel, Immunodominant T cell epitope from signal sequence, Science 257 (1992) 1142, https://doi.org/10.1126/science.257.5073.1142-a.

[45] E. Bahar, J.-Y. Kim, H. Yoon, Chemotherapy resistance explained through endoplasmic reticulum stress-dependent signaling, Cancers 11 (2019) 338, https://doi.org/10.3390/cancers11030338.
[46] S.J. Kierans, C.T. Taylor, Regulation of glycolysis by the hypoxia-inducible factor (HIF): implications for cellular physiology, J. Physiol. 599 (2021) 23–37, https://doi.org/10.1113/JP280572.
[47] D. Zhou, Z. Duan, Z. Li, F. Ge, R. Wei, L. Kong, The significance of glycolysis in tumor progression and its relationship with the tumor microenvironment, Front. Pharmacol. 13 (2022), https://doi.org/10.3389/FPHAR.2022.1091779.
[48] L. Zeng, S. Kizaka-Kondoh, S. Itasaka, X. Xie, M. Inoue, K. Tanimoto, K. Shibuya, M. Hiraoka, Hypoxia inducible factor-1 influences sensitivity to paclitaxel of human lung cancer cell lines under normoxic conditions, Cancer Sci. 98 (2007) 1394–1401, https://doi.org/10.1111/J.1349-7006.2007.00537.X.
[49] G. Raspaglio, F. Filippetti, S. Prislei, R. Penci, I. De Maria, L. Cicchillitti, S. Mozzetti, G. Scambia, C. Ferlini, Hypoxia induces class III beta-tubulin gene expression by HIF-1 alpha binding to its 3' flanking region, Gene 409 (2008) 100–108, https://doi.org/10.1016/J.GENE.2007.11.015.
[50] L. Flamant, A. Notte, N. Ninane, M. Raes, C. Michiels, Anti-apoptotic role of HIF-1 and AP-1 in paclitaxel exposed breast cancer cells under hypoxia, Mol. Cancer 9 (2010) 191, https://doi.org/10.1186/1476-4598-9-191.
[51] J.A. Yalowitz, H.N. Jayaram, Molecular targets of guanine nucleotides in differentiation, proliferation and apoptosis, Anticancer Res. 20 (2000) 2329–2338.
[52] E.W. Gerner, F.L. Meyskens, Polyamines and cancer: old molecules, new understanding, Nat. Rev. Cancer 4 (2004) 781–792, https://doi.org/10.1038/nrc1454.
[53] L. Arseni, R. Sharma, N. Mack, D. Nagalla, S. Ohl, T. Hielscher, M. Singhal, R. Pilz, H. Augustin, R. Sandhoff, C. Herold-Mende, B. Tews, P. Lichter, M. Seiffert, Sphingosine-1-Phosphate recruits macrophages and microglia and induces a pro-tumorigenic phenotype that favors glioma progression, Cancers 15 (2023) 479, https://doi.org/10.3390/cancers15020479.
[54] S. Mandal, A. Mandal, H.E. Johansson, A.V. Orjalo, M.H. Park, Depletion of cellular polyamines, spermidine and spermine, causes a total arrest in translation and growth in mammalian cells, Proc. Natl. Acad. Sci. U.S.A. 110 (2013) 2169–2174, https://doi.org/10.1073/pnas.1219002110.